Directional magnetoelectric effects in $MnWO_4$: magnetic sources of the electric polarization

2010 J. Phys.: Condens. Matter 22 065901

(http://iopscience.iop.org/0953-8984/22/6/065901)

IOP PUBLISHING JOURNAL OF PHYSICS: CONDENSED MATTER

J. Phys.: Condens. Matter **22** (2010) 065901 (6pp) doi:10.1088/0953-8984/22/6/065901

Directional magnetoelectric effects in $MnWO_4$: magnetic sources of the electric polarization

P Tolédano[1], B Mettout[1], W Schranz[2] and G Krexner[2]

[1] Laboratory of Physics of Complex Systems, University of Picardie, 33 rue Saint-Leu, 80000 Amiens, France
[2] Faculty of Physics, University of Vienna, Boltzmanngasse 5, A-1090 Vienna, Austria

E-mail: pierre.toledano@wanadoo.fr

Received 4 December 2009
Published 22 January 2010
Online at stacks.iop.org/JPhysCM/22/065901

Abstract
The ferroelectric order and magnetic field induced effects observed in the spiral phase of $MnWO_4$ are described theoretically. It is demonstrated explicitly that the Dzyaloshinskii–Moriya antisymmetric interactions contribute to the correlation between spins and electric dipoles in the incommensurate and commensurate ferroelectric phases of magnetic multiferroics. However, other single-site symmetric interactions are shown to be involved in the magnetoelectric process, suggesting the possible existence of an electric polarization originating from purely symmetric effects.

(Some figures in this article are in colour only in the electronic version)

1. Introduction

A typical feature of multiferroic materials undergoing a transition to an elliptic spiral ferroelectric phase [1–3], is the existence of spectacular magnetoelectric effects, such as the polarization flops observed in $TbMnO_3$ [4] and $DyMnO_3$ [5], or the sign reversal of P_y disclosed under magnetic field in $TbMn_2O_5$ [6]. The theoretical description of these effects requires knowledge of the order-parameter symmetry associated with the ferroelectric transition. In addition, the orientation of the applied magnetic field with respect to the magnetic spins influences the stability range of the spiral phase and the polarization-flop process. This property was recently illustrated by remarkable magnetic field induced effects observed in the ferroelectric phase of $MnWO_4$: the stability range of the phase depends on the direction of the applied field [7–10], which induces a high-field polarization-flop transition [11]. Here we show that these directional effects result from the order-parameter symmetry associated with the ferroelectric phase of $MnWO_4$, the stability of which depends on the respective orientations of the magnetic field and magnetic easy axis.

It is of fundamental interest to understand what is the microscopic mechanism behind the magnetoelectric coupling in multiferroics. It is generally believed [3], that in $RMnO_3$ (R = Tb, Dy, Gd) the *antisymmetric* Dzyaloshinskii–Moriya (DM) interaction is the microscopic origin for the ferroelectric polarization. For RMn_2O_5 the spins are almost collinear in the main ferroelectric phase and it is claimed [12] that *symmetric* exchange striction induces ferroelectricity. To gain insight into the microscopic mechanism for ferroelectricity in $MnWO_4$ we express the order parameters in terms of the magnetic spins and provide the correspondence between spins and electric dipoles. This analysis confirms that the Dzyaloshinskii–Moriya (DM) interactions [13, 14] contribute to the electric polarization in the incommensurate spiral phase but, additionally, shows that they participate as well in the formation of the dipole moments in the *commensurate* ferroelectric phases of magnetic multiferroics. We also find that the DM interaction is not the only microscopic source of the polarization: other *symmetric* interactions are shown to be involved in the magnetoelectric process, suggesting the possible existence of a polarization induced by purely symmetric effects.

2. P → AF3 → AF2 → AF1 transitions

Below its wolframite-type paramagnetic (P) structure, of monoclinic $P2/c1'$ symmetry, $MnWO_4$ undergoes three

Table 1. Generators of the irreducible corepresentations $\Gamma^{\mathbf{k}1}$ and $\Gamma^{\mathbf{k}2}$ of the $P2/c1'$ paramagnetic space group, deduced from the irreducible representations $\hat{\tau}_1$ and $\hat{\tau}_2$ of $G_k = m_y$, given in Kovalev's tables [15] for $\mathbf{k}_{\rm inc}$ and $\mathbf{k}_{\rm com}$. T is the time reversal symmetry. For AF2 and AF3, $\varepsilon \approx 0.457\pi$, $\varepsilon_1 \approx 0.418\pi$ and $\varepsilon_2 = 2\varepsilon$. For AF1, $\varepsilon = \varepsilon_1 = \pi/2$ and $\varepsilon_2 = \pi$.

$P2/c1'$		$(\sigma_y\|00\frac{c}{2})$	$(I\|000)$	T	$(E\|a00)$	$(E\|0b0)$	$(E\|00c)$
$\Gamma^{\mathbf{k}1}$	$\bar{S}_1$ $\bar{S}_1{}^*$	$\begin{pmatrix} e^{i\varepsilon} & \\ & e^{-i\varepsilon} \end{pmatrix}$	$\begin{pmatrix} & 1 \\ 1 & \end{pmatrix}$	$\begin{pmatrix} -1 & \\ & -1 \end{pmatrix}$	$\begin{pmatrix} e^{i\varepsilon_1} & \\ & e^{-i\varepsilon_1} \end{pmatrix}$	$\begin{pmatrix} -1 & \\ & -1 \end{pmatrix}$	$\begin{pmatrix} e^{i\varepsilon_2} & \\ & e^{-i\varepsilon_2} \end{pmatrix}$
$\Gamma^{\mathbf{k}2}$	$\bar{S}_2$ $\bar{S}_2{}^*$	$\begin{pmatrix} -e^{i\varepsilon} & \\ & -e^{-i\varepsilon} \end{pmatrix}$	$\begin{pmatrix} & 1 \\ 1 & \end{pmatrix}$	$\begin{pmatrix} -1 & \\ & -1 \end{pmatrix}$	$\begin{pmatrix} e^{i\varepsilon_1} & \\ & e^{-i\varepsilon_1} \end{pmatrix}$	$\begin{pmatrix} -1 & \\ & -1 \end{pmatrix}$	$\begin{pmatrix} e^{i\varepsilon_2} & \\ & e^{-i\varepsilon_2} \end{pmatrix}$

successive magnetic phase transitions [7, 8] at 13.5 K ($T_{\rm N}$), 12.7 K (T_2) and 7.6 K (T_1). They lead, respectively, to an incommensurate magnetic phase (AF3), an incommensurate elliptical spiral phase (AF2) displaying an electric polarization $\vec{P} \parallel b$, and a commensurate magnetic phase (AF1). The transition wavevectors [7] are $\mathbf{k}_{\rm inc} = (-0.214, \frac{1}{2}, 0.457)$ for AF2 and AF3, and $\mathbf{k}_{\rm com} = (\pm\frac{1}{4}, \frac{1}{2}, \frac{1}{2})$ for AF1. They are associated with two bidimensional irreducible corepresentations of the $P2/c1'$ space group [15], denoted by $\Gamma^{\mathbf{k}1}$ and $\Gamma^{\mathbf{k}2}$ in [7], whose generators are given in table 1.

The complex amplitudes transforming according to $\Gamma^{\mathbf{k}1}$ and $\Gamma^{\mathbf{k}2}$, which form the order-parameter components, are denoted by $\bar{S}_1 = S_1 e^{i\theta_1}$, $\bar{S}_1{}^* = S_1 e^{-i\theta_1}$ and $\bar{S}_2 = S_2 e^{i\theta_2}$, $\bar{S}_2{}^* = S_2 e^{-i\theta_2}$. For $\mathbf{k} = \mathbf{k}_{\rm inc}$ the order-parameter invariants $\Im_1 = S_1^2$, $\Im_2 = S_2^2$ and $\Im_3 = S_1^2 S_2^2 \cos(2\varphi)$, with $\varphi = \theta_1 - \theta_2$, yield the Landau expansion:

$$\Phi_1(T, S_1, S_2, \varphi) = \Phi_{10}(T) + \frac{\alpha_1}{2}S_1^2 + \frac{\beta_1}{4}S_1^4 + \frac{\alpha_2}{2}S_2^2 + \frac{\beta_2}{4}S_2^4 + \frac{\gamma_1}{2}S_1^2 S_2^2 \cos(2\varphi) + \frac{\gamma_2}{4}S_1^4 S_2^4 \cos^2(2\varphi) + \cdots. \quad (1)$$

Minimizing Φ_1 shows that five distinct stable states, denoted I–V, may arise below the P-phase for different equilibrium values of S_1, S_2 and φ, as summarized in figure 1(a). The theoretical phase diagram shown in figure 1(b) gives the location of the phases in the $(\gamma_1, \alpha_1 - \alpha_2)$ plane.

Neutron diffraction data [7] show that the incommensurate magnetic AF3 phase induced by $\Gamma^{\mathbf{k}2}$ corresponds to $S_1^{\rm e} = 0$ and $S_2^{\rm e} \neq 0$, coinciding with phase I in figure 1(a). Its structure has the antiferromagnetic grey point-group $2_y/m_y1'$, involving a doubling of the b-lattice parameter, and an incommensurate modulation of the spin density in the (x, z)-plane. The AF2 spiral phase, induced by $\Gamma^{\mathbf{k}1} + \Gamma^{\mathbf{k}2}$ [7], corresponds to phase II in figure 1(a) with $S_1^{\rm e} \neq 0$, $S_2^{\rm e} \neq 0$, $\varphi = (2n+1)\frac{\pi}{2}$ and the magnetic symmetry $2_y1'$. Adding the dielectric part of the free energy density $\Phi_1^{\rm D} = \delta P_y S_1 S_2 \sin\varphi + \frac{P_y^2}{2\varepsilon_{yy}^0}$ to equation (1) yields the equilibrium polarization

$$P_y^{\rm e} = \pm\delta\varepsilon_{yy}^0 S_1^{\rm e} S_2^{\rm e}, \quad (2)$$

which changes its sign for opposite senses of the spiral configuration, as observed by Sagayama *et al* [9]. The order-parameter $\bar{S}_2$, activated at the P → AF3 transition, is frozen at the AF3 → AF2 transition, i.e. independent of temperature below T_2. Therefore, equation (2) expresses a *linear* dependence of $P_y^{\rm e}$ on $\bar{S}_1^{\rm e}$, since $\delta\varepsilon_{yy}^0 S_1^{\rm e}$ acts as a temperature independent coupling coefficient.

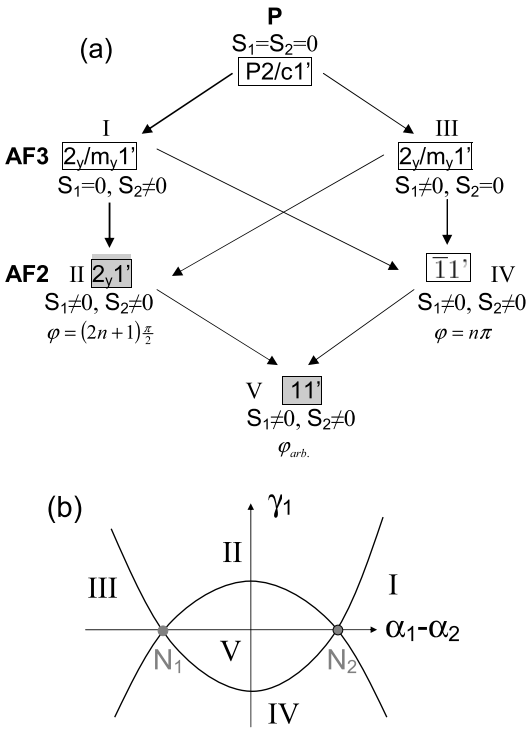

Figure 1. (a) Connections between the magnetic point groups of phases I–V induced by $\Gamma^{\mathbf{k}1} + \Gamma^{\mathbf{k}2}$ and equilibrium conditions fulfilled by the order parameter in each phase. Grey rectangles indicate ferroelectric phases. (b) Phase diagram deduced from the minimization of Φ_1 given in equation (1) in the $(\gamma, \alpha_1 - \alpha_2)$-plane. The phases are separated by second-order transition curves crossing at the four-phase points N_1 and N_2.

In the AF2 and AF3 phases Φ_1 can be truncated at the fourth degree, since the eighth degree invariant is necessary only for stabilization of phase V (of figure 1(a)). Putting $\alpha_1 = a_1(T - T_0)$ and $\alpha_2 = a_2(T - T_{\rm N})$ and minimizing Φ_1 of equation (1) with respect to S_1 and S_2 one obtains the equilibrium values for the order-parameter components $S_1^{\rm e}$ and $S_2^{\rm e}$.

AF3 ($T_2 < T < T_{\rm N}$) corresponds to

$$S_1^{\rm e} = 0 \qquad \text{and} \qquad S_2^{\rm e} = \pm\left[\frac{a_2}{\beta_2}(T_{\rm N} - T)\right]^{1/2}. \quad (3)$$

For $T \leqslant T_2$ (AF2 phase) one obtains

$$S_1^{\rm e} = \pm\tilde{a}(T_2 - T)^{1/2} \qquad \text{and} \qquad S_2^{\rm e} = \pm\left[\frac{\alpha_2}{\beta_2}(T_{\rm N} - T_2)\right]^{1/2} \quad (4)$$

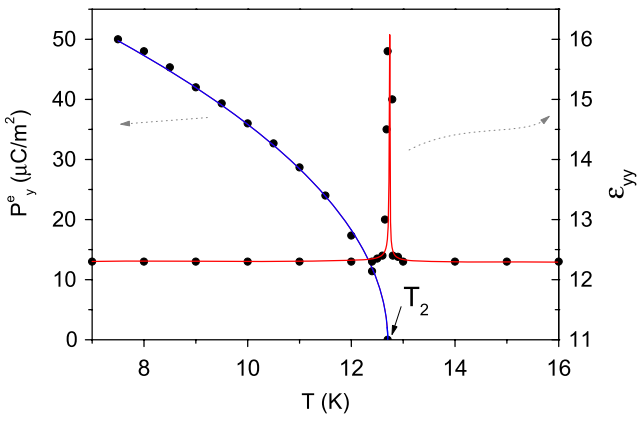

Figure 2. Fit (lines) of the temperature dependence of the spontaneous polarization $P^e_y(T)$ and the dielectric permittivity $\varepsilon_{yy}(T)$ using equations (6) and (7). The points are data from Taniguchi *et al* [8]. The fit parameters are $A = 21.8\ \mu\text{C m}^{-2}\ \text{K}^{-1/2}$, $C = 0.001$, $D = 0.0001$ and $\varepsilon^0_{yy} = 12.3$.

with

$$\tilde{a} = \left(\frac{a_2\gamma_1 + a_1\beta_2}{\beta_1\beta_2 - \gamma_1^2}\right)^{1/2} \quad \text{and} \qquad T_2 = \frac{a_2\gamma_1 T_\text{N} + a_1\beta_2 T_0}{a_2\gamma_1 + a_1\beta_2}. \tag{5}$$

Inserting equation (4) into (2) one finds that the spontaneous polarization in the AF2 phase varies as

$$P^e_y(T) = \pm A(T_2 - T)^{1/2} \tag{6}$$

with $A = \delta\varepsilon^0_{yy}\tilde{a}[\frac{a_2}{\beta_2(T_\text{N}-T_2)}]^{1/2}$. The dielectric permittivity follows a Curie–Weiss-type law around T_2 with

$$\varepsilon_{yy}(T) = \varepsilon^0_{yy}\left[1 - C\frac{T_\text{N} - T}{T - T_2}\right] \quad \text{for } T > T_2$$
$$\varepsilon_{yy}(T) = \varepsilon^0_{yy}\left[1 - D\frac{T_\text{N} - T_2}{T_2 - T}\right] \quad \text{for } T < T_2 \tag{7}$$

where $C = \frac{\delta^2 a_2 \varepsilon^0_{yy}}{a_2\gamma_1 + a_1\beta_2}$ and $D = C\frac{\gamma_1^2 - \beta_1\beta_2}{\gamma_1^2 - 4\beta_1\beta_2}$.

Figure 2 shows that $P^e_y(T)$ and $\varepsilon_{yy}(T)$ perfectly fit the experimental curves reported by Taniguchi *et al* [8]. This confirms the hybrid character of the ferroelectricity in spiral magnets, recently found [17, 18] also for $TbMnO_3$ and $TbMn_2O_5$: the square-root temperature dependence of the polarization (equation (6)) and the Curie–Weiss-type behaviour of ε_{yy} expressed by equation (7) are typical for a *proper* ferroelectric transition, whereas the low value of $P_y \approx 40\ \mu\text{C m}^{-2}$ measured at 10 K [16] is of the order found in *improper* ferroelectrics.

Let us now turn to the AF1 phase. Neutron diffraction results [7] indicate that the transition to the commensurate AF1 phase triggers a *decoupling* of $\bar{S}_1$ and $\bar{S}_2$. Using table 1 one finds that the lock-in at T_1, induced by $\Gamma^{\mathbf{k}2}$, gives rise to the additional invariant $\Im_4 = S_2^4\cos(4\theta_2)$. The Landau expansion associated with the transition to AF1 is

$$\Phi_2(T, S_2, \theta_2) = \Phi_{20}(T) + \frac{\alpha'}{2}S_2^2 + \frac{\beta'}{4}S_2^4 + \frac{\gamma_1'}{4}S_2^4\cos(4\theta_2) + \frac{\gamma_2'}{8}S_2^8\cos^2(4\theta_2). \tag{8}$$

The equations of state show that three commensurate phases, denoted by I′-to-III′, displaying a fourfold increased unit cell ($\mathbf{b}+\mathbf{c}$, $\mathbf{c}-\mathbf{b}$, $\mathbf{2a}+\mathbf{c}$), may appear below T_1. The AF1 phase corresponds to phases I′ or II′, stable for $\cos(4\theta_2^e) = +1$ or -1, respectively, both described by the magnetic space group C_a2/c. Phase III′, stable for $\cos(4\theta_2^e) = \frac{\gamma_1'\beta'^2}{\gamma_2'\alpha'^2}$, has the symmetry C_ac.

3. Directional magnetic field (magnetoelectric) effects

The AF1 and AF2 order parameters allow the description of the magnetoelectric effects [8–11, 19] observed in $MnWO_4$. The magnetic phase diagram can be calculated by adding the magnetic part of the free energy and the coupling invariants $\kappa_i M_i^2 S_1^2 + \kappa_i' M_i^2 S_2^2$

$$\Phi_1^M = \tfrac{1}{2}\vec{M}\hat{\mu}\vec{M} - \vec{B}\vec{M} + \kappa_i M_i^2 S_1^2 + \kappa_i' M_i^2 S_2^2 \tag{9}$$

to the Landau expansion equation (1) or (8). $\hat{\mu}$ is the paramagnetic susceptibility tensor and $i = x, y, z$.

Due to the anisotropy of the magnetic free energy, the AF2 stability range depends on the angle $\Psi_0 = \frac{1}{2}\tan^{-1}[2\mu_{xz}(\mu_{zz} - \mu_{xx})^{-1}]$ between $\vec{B}$ and the magnetic easy axis in the paramagnetic phase. If $\vec{B}$ is at an angle Ψ with the x-axis, one finds

$$T_2(\Psi) - T_2 = \varepsilon B^2\left\{1 - \frac{td^{-1}}{2}\left[t - \sqrt{t^2 - 4d}\cos 2(\Psi - \Psi_0)\right]\right\} \tag{10}$$

where $\varepsilon = (\beta_1\kappa + \gamma_1\kappa')(\beta_1\alpha_1 + \gamma_1\alpha_2)^{-1}$, $t = \mu_{xx} + \mu_{zz}$ and $d = \mu_{xx}\mu_{zz} - \mu_{xz}^2$. For $\varepsilon < 0$ the AF2 stability range is maximum for $\vec{B}$ along the easy axis ($\Psi = \Psi_0$). It decreases when Ψ increases from Ψ_0 to $\Psi_0 + \pi/2$, reducing to the stability range at zero field if $\mu_{xz}, \mu_{xx} << \mu_{zz}$. Such a variation has been observed in the AF2 phase [10, 20, 21], in which $\Psi_0 \approx 35°$ coincides with the direction of the spins in the $(x.z)$-plane. When $\vec{B}$ is at an angle ψ with the (x, z)-plane the AF2 stability range decreases when ψ increases from $\psi = 0$ to $\psi = \pi/2$, as reported experimentally [10, 20].

To get an overview about the magnetic field dependence of the various phases in $MnWO_4$ it may be useful to consider a simplified version of the free energy expansion by neglecting the non-diagonal parts of $\hat{\mu}$. Then, by minimizing the free energy with respect to M_i one obtains for the magnetization in x, y or z-direction

$$M_i = \frac{B_i}{\mu_i + \kappa_i S^2} \tag{11}$$

and the phase transition temperatures are shifted under applied magnetic field B_i as

$$T_\alpha(B_i) = T_\alpha(0) - \frac{\kappa_i}{a\mu_i^2}B_i^2 \tag{12}$$

where $T_\alpha := T_1, T_2$ or T_N and $a > 0$ is the bare expansion coefficient of the second-order term in equation (1). Equation (12) shows, that the phase transition temperatures depend quadratically on the applied magnetic field and the sign

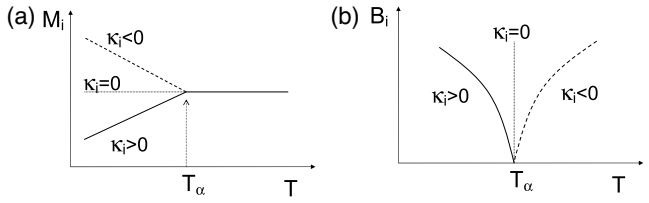

Figure 3. Magnetizations M_i (a) and magnetic field dependence (b) of transition temperatures calculated from equations (11) and (12).

of the magnetic field shift of T_α depends only on the sign of the coupling coefficient κ_i, which itself can be determined from the changes of M_i with temperature (see equation (11)). Figure 3 sketches this behaviour.

Equations (11) and (12) describe the magnetic phase diagram (see e.g. figure 5 of [20]) perfectly. The strongest downshift of T_1 occurs in the x-direction, which also corresponds to the strongest negative anomaly in M_x at T_1, implying $\kappa_x \gg \kappa_z > 0$ as seen from figure 3 of [20]. This figure also shows that $\kappa_y < 0$ at T_1 (M_y displays an upwards anomaly at T_1) and therefore $T_1(B_y)$ increases with applied magnetic field. In this way all the particular features of the phase diagram can be reproduced.

In the following we will briefly discuss the effect of a very high magnetic field B_y. Above a threshold field $B_y^{\rm th}$, given by $\Phi_1(T_1, S_1^{\rm e}, S_2^{\rm e}) - B_y^{\rm th} M_y^{\rm II} = \Phi_2(T_1, S_2^{\rm e}) - B_y^{\rm th} M_y^{\rm III'}$, the AF2 phase switches to the high-field phase III′, which cancels P_y and gives rise to the polarization:

$$P_x^{\rm III'} = -\delta' \varepsilon_{xx}^0 S_2^{\rm e2} \sin(2\theta_2^{\rm e}) \tag{13}$$

deduced from the dielectric free energy $\Phi_2^{\rm D} = \delta' P_x S_2^2 \sin(2\theta_2) + \frac{P_x^2}{2\varepsilon_{xx}^0}$. The onset of $P_x^{\rm III'}$ occurs in correlation with the vanishing of $P_y^{\rm e}$ at the first-order AF2 $\rightarrow$ III′ flop transition, consistent with the $P_y \rightarrow P_x$ polarization flop [8] observed above 10 T. Decreasing B_y below $B_y^{\rm th}$ switches back phase III′ to AF2. If B_y is canted at an angle ϕ with respect to the b-axis in the (x, z)-plane, the magnetoelectric coupling $\nu P_x M_x M_y S_1 S_2 \sin\varphi$ induces the polarization

$$P_x^{\rm e} = -\varepsilon_{yy}^0 \nu \mu_{yy}^{-2} B_y^2 S_1^{\rm e} S_2^{\rm e} \sin\varphi^{\rm e} \sin 2\phi. \tag{14}$$

Canting B_y oppositely from the b-axis ($\phi \rightarrow -\phi$) *reverses* $P_x^{\rm e}$. Increasing again B_y above $B_y^{\rm th}$ yields an *opposite sign* for $P_x^{\rm III'}$ in phase III′, as observed by Taniguchi *et al* [11].

4. Relating the order parameters to magnetic spins

To gain insight into the nature of the microscopic interactions, let us express $\bar{S}_1$ and $\bar{S}_2$ as a function of the magnetic spins in the commensurate phases I′–III′. Denoting $\mathbf{s_1}$–$\mathbf{s_8}$ the spins associated with the eight Mn^{2+}-ions of the corresponding fourfold primitive monoclinic unit cell, one can write $\mathbf{s_i} = s_i^a \vec{a} + s_i^b \vec{b} + s_i^c \vec{c}$ (i = 1–8), where $\vec{a}$, $\vec{b}$ and $\vec{c}$ are lattice vectors. Projecting on $\Gamma^{\mathbf{k}1}$ and $\Gamma^{\mathbf{k}2}$ the matrices transforming the $s_i^{a,b,c}$-components gives

$$\begin{aligned} \bar{S}_1^{\,a,c} &= L_1^{a,c} + {\rm i} L_3^{a,c} & \bar{S}_1^{\,b} &= -L_4^b + {\rm i} L_2^b \\ \bar{S}_2^{\,a,c} &= -L_4^{a,c} + {\rm i} L_2^{a,c} & \bar{S}_2^{\,b} &= L_1^b + {\rm i} L_3^b \end{aligned} \tag{15}$$

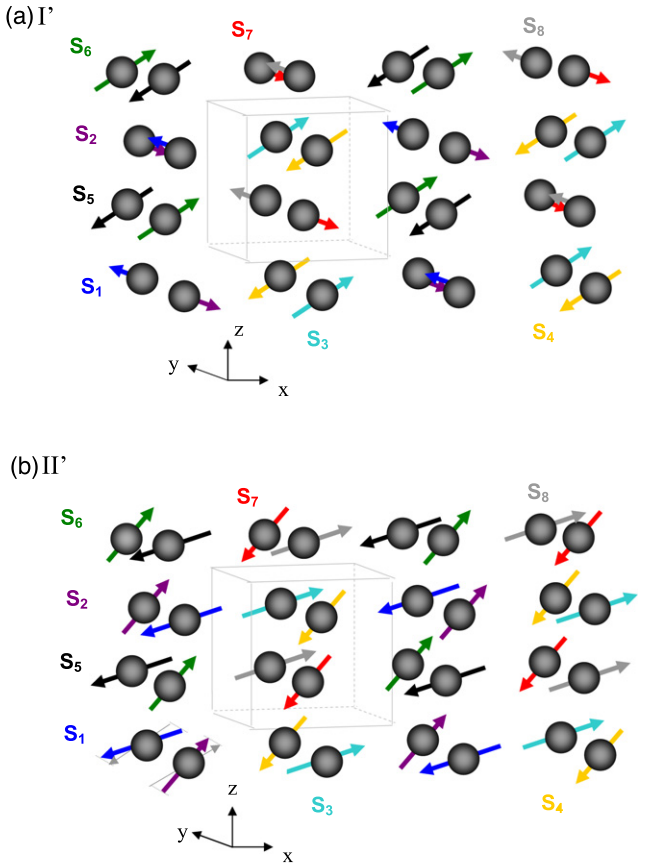

Figure 4. Calculated magnetic structures of (a) phase I′ and (b) phase II′, described in the text. The two additional grey arrows oriented in (x, z)-plane located at the two atoms in the bottom left of (b) indicate the previously refined [7] magnetic structure of the AF1 phase. The coordinates of the eight Mn^{2+} ions, corresponding to the spins $\mathbf{s}_1 - \mathbf{s}_8$, in the primitive monoclinic unit cell of the two structures are for ion $1(\frac{1}{2}, y-1, \frac{5}{4})$, $2(\frac{1}{2}, y, \frac{5}{4})$, $3(\frac{3}{2}, y, \frac{5}{4})$, $4(\frac{3}{2}, y, \frac{9}{4})$, $5(\frac{1}{2}, \bar{y}, \frac{3}{4})$, $6(\frac{1}{2}, \bar{y}, \frac{7}{4})$, $7(\frac{3}{2}, \bar{y}, \frac{7}{4})$, $8(\frac{3}{2}, 1-y, \frac{7}{4})$.

where the $\bar{S}_i^{\,m}$ (i = 1, 2 $m = a$, b, c) represent different forms of $\bar{S}_1$ and $\bar{S}_2$. The L_i^m (i = 1–4) are projections of the vectors

$$\begin{aligned} \mathbf{L_1} &= \mathbf{s_1} - \mathbf{s_2} - \mathbf{s_7} + \mathbf{s_8} & \mathbf{L_2} &= \mathbf{s_1} - \mathbf{s_2} + \mathbf{s_7} - \mathbf{s_8} \\ \mathbf{L_3} &= \mathbf{s_3} - \mathbf{s_4} + \mathbf{s_5} - \mathbf{s_6} & \mathbf{L_4} &= \mathbf{s_3} - \mathbf{s_4} - \mathbf{s_5} + \mathbf{s_6}. \end{aligned} \tag{16}$$

In phase I′ ($\bar{S}_1^{\,a,b,c} = 0, \cos 4\theta_2^{a,b,c} = 1$) one has $s_1^{a,c} = s_2^{a,c} = s_7^{a,c} = s_8^{a,c} = 0$, $s_3^b = s_4^b = s_5^b = s_6^b = 0$, $s_3^{a,c} = -s_4^{a,c} = -s_5^{a,c} = s_6^{a,c}$ and $s_1^b = -s_2^b = -s_7^b = s_8^b$. It gives $\bar{S}_2^{\,a,c} = -L_4^{a,c}$ and $\bar{S}_2^{\,b} = L_1^b$.

In phase II′ ($\bar{S}_1^{\,a,b,c} = 0, \cos 4\theta_2^{a,b,c} = -1$) $s_1^{a,c} = -s_2^{a,c} = s_7^{a,c} = -s_8^{a,c} = -s_3^{a,c} = s_4^{a,c} = s_5^{a,c} = -s_6^{a,c}$ and $s_1^b = -s_2^b = -s_7^b = s_8^b = s_3^b = -s_4^b = s_5^b = -s_6^b$. It yields $\bar{S}_2^{\,a,c} = -L_4^{a,c} + {\rm i} L_2^{a,c}$ and $\bar{S}_2^{\,b} = L_1^b + {\rm i} L_3^b$.

Figures 4(a) and (b) show that the magnetic structure of the AF1 phase of $MnWO_4$ *coincides with the antiferromagnetic order of phase* II′ (figure 4(b)), since the cancellation of the (a, c)-spin-components on the sites 1, 2, 7 and 8 in phase I′ (figure 4(a)) was not observed [7] in AF1. The lack of spin components along $\vec{b}$ reported in this phase [7] may be due to their relativistic origin, as suggested in [7]. In phase III′

($\bar{S_1}^{a,b,c} = 0, \theta_2^{a,b,c} \neq 0, \pi/4$), identified as the high-field phase of $MnWO_4$, the equilibrium spins are $s_1^{a,c} = -s_2^{a,c} = s_7^{a,c} = -s_8^{a,c}$, $s_3^{a,c} = -s_4^{a,c} = -s_5^{a,c} = s_6^{a,c}$, $s_1^b = -s_2^b = s_7^b = -s_8^b$ and $s_3^b = -s_4^b = s_5^b = -s_6^b$, with $\bar{S_2}^{a,c} = -L_4^{a,c} + \mathrm{i}L_2^{a,c}$ and $\bar{S_2}^b = \mathrm{i}L_3^b$.

Other commensurate structures can take place for $\mathbf{k} = \mathbf{k}_{\mathrm{com}}$ when the spin components associated with $\bar{S}_1$ and $\bar{S}_2$ order simultaneously. Two among these structures, denoted IV′ ($\theta_1^e = 0, \theta_2^e = \pi/2$) and V′ ($\theta_1^e = \pi/2, \theta_2^e = 0$), display the symmetry 2_y and the same form of $P_y \propto \frac{1}{2\mathrm{i}}(\bar{S}_1\bar{S}_2^* - \bar{S}_2\bar{S}_1^*) = S_1S_2\sin\varphi$ as in the AF2 phase. Although these structures are not stabilized in $MnWO_4$, they are lock-in limits of the incommensurate AF2 structure, and can be used for investigating the microscopic origin of ferroelectricity in the spiral magnetic structure. Since $\bar{S}_1$ and $\bar{S}_2$ are both realized by three independent combinations of spin components, and taking into account the equilibrium relationships $\mathbf{s}_1 = -\mathbf{s}_2$, $\mathbf{s}_3 = -\mathbf{s}_4$, $\mathbf{s}_5 = -\mathbf{s}_6$ and $\mathbf{s}_7 = -\mathbf{s}_8$, which hold for all commensurate structures of $MnWO_4$, P_y is expressed as the sum of nine terms:

$$\begin{aligned}P_y = {} & \delta_1(s_1^{a2} + s_3^{a2} - s_5^{a2} - s_7^{a2}) + \delta_2(s_1^{b2} + s_3^{b2} - s_5^{b2} - s_7^{b2}) \\ & + \delta_3(s_1^{c2} + s_3^{c2} - s_5^{c2} - s_7^{c2}) \\ & + \delta_4(s_1^a s_1^c + s_3^a s_3^c - s_5^a s_5^c - s_7^a s_7^c) \\ & + \delta_5(s_1^b s_5^a - s_1^a s_5^b + s_3^b s_7^a - s_3^a s_7^b) \\ & + \delta_6(s_1^b s_5^c - s_1^c s_5^b + s_3^b s_7^c - s_3^c s_7^b) \\ & + \delta_7(s_1^b s_3^a - s_1^a s_3^b + s_5^b s_7^a - s_5^a s_7^b) \\ & + \delta_8(s_1^b s_3^c - s_1^c s_3^b + s_5^b s_7^c - s_5^c s_7^b) \\ & + \delta_9(s_3^a s_5^c - s_3^c s_5^a + s_1^c s_7^a - s_1^a s_7^c). \end{aligned} \tag{17}$$

The δ_1–δ_4 terms in equation (17) are symmetric invariants involving a single atom. Their origin is entropic and due to on-site interactions. The δ_5–δ_9 terms represent Dzyaloshinskii–Moriya (DM) antisymmetric coupling interactions between neighbouring pairs of spins $\mathbf{s}_1, \mathbf{s}_5$ (or the equivalent pair $\mathbf{s}_3, \mathbf{s}_7$), $\mathbf{s}_1, \mathbf{s}_3$ ($\mathbf{s}_5, \mathbf{s}_7$) and $\mathbf{s}_3, \mathbf{s}_5$ ($\mathbf{s}_1, \mathbf{s}_7$). The DM interaction [22, 23] is currently assumed to be the microscopic source of the polarization in the spiral structure of magnetic multiferroics [11, 13]. Our results explicitly confirm this view in $MnWO_4$, but show that other *symmetric* effects are also involved in the formation of the electric dipoles. Furthermore, equilibrium relationships of the spin components in phases IV′ ($s_1^b = s_7^b = 0, s_3^{a,c} = s_5^{a,c} = 0$) and V′ ($s_3^b = s_5^b = 0, s_1^{a,c} = s_7^{a,c} = 0$) preserve the symmetric and DM contributions in equation (17). This indicates that the interactions giving rise to the polarization in the commensurate ferroelectric phases of multiferroic compounds are of the same nature as in the spiral phases. The effect of the incommensurability in the x–z plane of the AF2 phase should result in further averaging of the spin densities without modifying essentially the invariants in equation (17). One should note that the DM interactions, as well as the Katsura-type contribution [13] $\mathbf{e}_{ij} \times \mathbf{s}_i \times \mathbf{s}_j$ (where $\mathbf{e}_{ij}$ is the distance vector joining neighbouring Mn atoms i and j), cancel in equation (17) when all spin components are cancelled except s_1^a and s_7^a in phase IV′, or s_3^a and s_5^a in phase V′, P_y keeping a finite value $P_y = \delta_1(s_1^{a2} - s_7^{a2})$ and $P_y = \delta_1(s_3^{a2} - s_5^{a2})$ in phases IV′ and V′, respectively. Therefore symmetry considerations predict the existence of a polarization induced by interactions being neither of Dzyaloshinskii–Moriya nor of Katsura-type, although such effects may encounter considerable restrictions at the microscopic level.

5. Summary and conclusion

In summary, the present work clarifies the nature of the ferroelectric order occurring in the spiral phase of $MnWO_4$, and gives a theoretical description of the field induced effects observed in this compound. It confirms that the antisymmetric Dzyaloshinskii–Moriya interaction is involved in the formation of dipolar moments in the incommensurate and commensurate ferroelectric structures of magnetic multiferroics. It also shows that other symmetric effects participate in the ferroelectricity observed in these compounds, suggesting the possible existence of an unconventional ferroelectricity in magnetoelectric materials originating from purely symmetric interactions. Symmetric exchange interactions may mediate magnetoelectric coupling in the E-type commensurate perovskite manganese oxide compounds [24]. For these materials a large ferroelectric polarization was predicted [25, 26] and recently found in $TmMnO_3$ [24].

Our theoretical description of the magnetoelectric effects in $MnWO_4$ differs in important aspects from the theoretical approach to this compound proposed by Harris [27]. We determine, from pure symmetry considerations, the irreducible degrees of freedom (corepresentations) involved in the observed sequence of phases, the corresponding order-parameter symmetries and the form of the transition free energies and related magnetic, dielectric and coupling contributions, which allow the description of the observed magnetoelectric effects. Finally, we take into account the actual positions of the Mn ions in order to establish the connection existing between our phenomenological order parameters and the magnetic spins or electric dipoles. Harris follows an opposite procedure, starting from the actual magnetic structure, which permits construction of allowed spin functions. These functions are then related to the order-parameter components, the transition free energy and coupling to the polarization being deduced from semi-empirical considerations. The advantage of our approach is that it provides the full set of stable states allowed by the order-parameter symmetries (one of which is stabilized under high magnetic field), a detailed topology of the corresponding phase diagram, a faithful description of the critical behaviour, including the specific pseudo-proper (not improper) character of the induced polarization [17], which had been overlooked by Harris. It also yields a precise explanation of the various magnetoelectric effects observed in $MnWO_4$ (not described by Harris) and an explicit determination of the different types of interactions contributing to the polarization.

Acknowledgments

We acknowledge support from the Austrian FWF (P19284-N20) and the University of Vienna through the Focus Research Area *Materials Science*.

References

[1] Fiebig M 2005 *J. Phys. D: Appl. Phys.* **38** R123
[2] Kimura T 2007 *Annu. Rev. Mater. Res.* **37** 387
[3] Cheong S W and Mostovoy M 2007 *Nat. Mater.* **6** 13
[4] Kimura T, Goto T, Shintani H, Ishizaka K, Arima T and Tokura Y 2003 *Nature* **426** 56
[5] Strempfer J, Bohnenbuck B, Mostovoy M, Aliouane N, Argyriou D N, Schrettle F, Hemberger J, Krimmel A and v Zimmermann M 2007 *Phys. Rev.* B **75** 212402
[6] Hur N, Park S, Sharma P A, Ahn J S, Guha S and Cheong S W 2004 *Nature* **429** 392
[7] Lautenschläger G, Weitzel H, Vogt T, Hock R, Böhm A, Bonnet M and Fuess H 1993 *Phys. Rev.* B **48** 6087
[8] Taniguchi K, Abe N, Takenobu T, Iwasa Y and Arima T 2006 *Phys. Rev. Lett.* **97** 097203
[9] Sagayama H, Taniguchi K, Abe N, Arima T, Soda M, Matsuura M and Hirota K 2008 *Phys. Rev.* B **77** 220407
[10] Taniguchi K, Abe N, Sagayama H, Ohtani S, Takenobu T, Iwasa Y and Arima T 2008 *Phys. Rev.* B **77** 064408
[11] Taniguchi K, Abe N, Umetsu H, Aruga Katori H and Arima T 2008 *Phys. Rev. Lett.* **101** 207205
[12] Sushkov A B, Mostovoy M, Aguilar R V, Cheong S W and Drew H D 2008 *J. Phys.: Condens. Matter* **20** 434210
[13] Katsura H, Nagaosa N and Balatsky A V 2005 *Phys. Rev. Lett.* **95** 057205
[14] Sergienko I A and Dagotto E 2006 *Phys. Rev.* B **73** 094434
[15] Kovalev O V 1965 *The Irreducible Representations of Space Groups* (New York: Gordon and Breach)
[16] Kundys B, Simon C and Martin C 2008 *Phys. Rev.* B **77** 172402
[17] Tolédano P 2009 *Phys. Rev.* B **79** 094416
[18] Tolédano P, Schranz W and Krexner G 2009 *Phys. Rev.* B **79** 144103
[19] Mitamura H, Kimura T, Sakakibara T and Kindo K 2009 *J. Phys.: Conf. Ser.* **150** 042126
[20] Arkenbout A H, Palstra T T M, Siegrist T and Kimura T 2006 *Phys. Rev.* B **74** 184431
[21] Chaudhury R P, Lorenz B, Wang Y Q, Sun Y Y and Chu C W 2008 *Phys. Rev.* B **77** 104406
[22] Dzyaloshinskii I E 1957 *Sov. Phys.—JETP* **5** 1259
[23] Moriya T 1960 *Phys. Rev.* **120** 91
[24] Pomjakushin V Yu, Kenzelmann M, Dönni A, Harris A B, Nakajima T, Mitsuda S, Tachibana M, Keller L, Mesot J, Kitazawa H and Takayama-Muromachi E 2009 *New J. Phys.* **11** 043019
[25] Sergienko I A, Sen C and Dagotto E 2006 *Phys. Rev. Lett.* **97** 227204
[26] Picozzi S, Yamauchi K, Sanyal B, Sergienko I A and Dagotto E 2007 *Phys. Rev. Lett.* **99** 227201
[27] Harris A B 2007 *Phys. Rev.* **76** 054447